NIH Public Access
Author Manuscript
Biomaterials. Author manuscript; available in PMC 2008 December 1.

Published in final edited form as:
Biomaterials. 2007 December ; 28(35): 5225–5237.

Diffusion of Vitamin E in Ultra-high Molecular Weight Polyethylene

Ebru Oral[a,b], **Keith K. Wannomae**[a], **Shannon L. Rowell**[a], and **Orhun K. Muratoglu**[a,b]

a *Massachusetts General Hospital, Department of Orthopaedic Surgery*

b *Harvard Medical School*

Abstract

Vitamin E-doped, radiation cross-linked ultra-high molecular weight polyethylene (UHMWPE) is developed as an alternate oxidation and wear resistant bearing surface in joint arthroplasty. We analyzed the diffusion behavior of vitamin E through UHMWPE and predicted penetration depth following doping with vitamin E and subsequent homogenization in inert gas used to penetrate implant components with vitamin E. Cross-linked UHMWPE (65- and 100-kGy irradiation) had higher activation energy and lower diffusion coefficients than uncross-linked UHMWPE, but there were only slight differences in vitamin E profiles and penetration depth between the two doses. By using homogenization in inert gas below the melting point of the polymer following doping in pure vitamin E, the surface concentration of vitamin E was decreased and vitamin E stabilization was achieved throughout a desired thickness. We developed an analytical model based on Fickian theory that closely predicted vitamin E concentration as a function of depth following doping and homogenization.

Keywords

vitamin E; highly cross-linked polyethylene; joint arthroplasty

Introduction

Ultra high molecular weight polyethylene (UHMWPE) has been the material of choice for the load bearing and articulating components in total joint arthroplasty [1]. Adhesive/abrasive wear of UHMWPE [2,3] has been the leading cause of peri-prosthetic osteolysis [4,5], compromising long-term performance of total joints. One method of improving the wear resistance of UHMWPE is radiation cross-linking [6–8]. Radiation cross-linking to a dose of 100 kGy has been shown to decrease adhesive/abrasive wear substantially in both in vitro experiments and in vivo clinical studies [9–11].

Highly cross-linked, wear resistant UHMWPEs currently in clinical use are prepared by irradiation and subsequent thermal treatment. The latter is used to decrease or eliminate the residual free radicals caused by irradiation. The residual free radicals are typically trapped in the crystalline regions and cause oxidative embrittlement in the long-term [12]. Melting of irradiated UHMWPE decreases the concentration of residual free radicals to undetectable levels and such components have been shown to be oxidation resistant both in vivo and in vitro

Corresponding Author: Orhun K. Muratoglu, Ph.D., Massachusetts General Hospital, 55 Fruit Street, GRJ-1206, Boston, MA 02114, (617) 726-3869 (voice) (617) 643-2521 (fax), omuratoglu@partners.org.

Publisher's Disclaimer: This is a PDF file of an unedited manuscript that has been accepted for publication. As a service to our customers we are providing this early version of the manuscript. The manuscript will undergo copyediting, typesetting, and review of the resulting proof before it is published in its final citable form. Please note that during the production process errors may be discovered which could affect the content, and all legal disclaimers that apply to the journal pertain.

NIH-PA Author Manuscript
NIH-PA Author Manuscript
NIH-PA Author Manuscript

NIH-PA Author Manuscript

NIH-PA Author Manuscript

NIH-PA Author Manuscript

[13]. One disadvantage of melting is the decrease in the crystallinity of irradiated polymer, which also decreases some of its mechanical properties [14].

We recently advanced an alternate method of preventing oxidation in irradiated UHMWPE through the stabilization of the residual free radicals with the antioxidant vitamin E (α-tocopherol) [15,16]. Vitamin E stabilization replaces post-irradiation melting and hence prevents the loss of crystallinity without sacrificing wear or oxidation resistance [17]. Vitamin E is a natural lipid whose major role *in vivo* is to donate a hydrogen atom to free radicals formed on lipids to hinder lipid peroxidation in cell membranes [18,19]. Its lipophilicity, due to its phytyl tail (Fig 1), allows it to penetrate through cell membranes, and also provides miscibility with polyethylene.

There are two methods of incorporating vitamin E into UHMWPE. One is to blend vitamin E with UHMWPE powder prior to consolidation. Once consolidated, the blend can be cross-linked with the use of ionizing radiation. However, the presence of vitamin E in UHMWPE during irradiation reduces the efficiency of cross-linking [20,21]. An alternative method is the diffusion of vitamin E into UHMWPE following radiation cross-linking [15,16]. The cross-linking efficiency of UHMWPE is not adversely affected in this method since vitamin E is not present during irradiation.

Therefore, it is desirable to study the diffusion of vitamin E in cross-linked UHMWPE. The molecular weight of this linear polyolefin is typically on the order of $1–6 \times 10^6$ grams per mole. The long chains of UHMWPE allow a 50–60% semi-crystalline structure with crystallites exhibiting a peak melting transition of approximately 135°C when crystallized from the melt at low pressures. These crystallites are impermeable to even small molecules such as oxygen and hence, would be impermeable to a relatively large molecule like α-tocopherol (430.7 g/mol). Therefore, the diffusion of vitamin E in polyethylene is primarily through the amorphous phase.

Diffusion through a semi-crystalline polymer cannot be characterized and predicted solely as diffusion through an amorphous volume because crystalline regions are expected to hinder the diffusion of molecules also by restricting diffusion pathways. Therefore, the diffusion coefficient of the amorphous region would be decreased due to impedance created by the crystallites. Since crystals start melting at about 100°C in UHMWPE (Fig 2), the impedance of crystallites are expected to decrease with increasing temperature above 100°C until the peak melting point at about 135°C. Likewise, chemical cross-links introduced into the amorphous phase are expected to decrease diffusion provided that chain scission as a result of irradiation has not decreased the molecular weight.

In order to interact with the residual free radicals and prevent oxidation, vitamin E has to be present throughout an irradiated UHMWPE joint implant [22] without detrimentally affecting morphological and mechanical properties. The diffusion of vitamin E in UHMWPE has not been extensively studied. Wolf et al. [23] have shown that vitamin E penetration through cross-linked UHMWPE can be achieved by using doping in pure vitamin E and further homogenization in inert atmosphere and supercritical carbon dioxide at temperatures above the melting point of cross-linked UHMWPE. This does not take into account the effect of the crystalline regions of UHMWPE, which need to be preserved during vitamin E stabilization to maintain the mechanical properties of cross-linked UHMWPE [14–16].

We studied the diffusion behavior of virgin and radiation-crosslinked UHMWPE as a function of temperature and time. We first tested the hypothesis that the diffusion through irradiated UHMWPEs would be hindered due to increased cross-link density. Furthermore, we studied the effects of a subsequent homogenization step in inert atmosphere below the melting point in diffusing a high surface concentration of vitamin E throughout a desired thickness of

NIH-PA Author Manuscript

NIH-PA Author Manuscript

NIH-PA Author Manuscript

UHMWPE. We developed an analytical model for the diffusion of vitamin E in UHMWPE to predict diffusion times to penetrate desired diffusion path lengths.

Experimental Section

Radiation cross-linking

Slab compression molded GUR1050 UHMWPE (Orthoplastics, Lancashire, UK) was packaged in aluminum foil packaging (5610, Technipaq, Inc., Crystal Lake, IL) in vacuum and irradiated to 65- and 100 kGy using ^{60}Co gamma irradiation (Steris Isomedix, Northborough, MA). Unirradiated virgin UHMWPE was used as a control.

Determination of cross-link density

Cross-link density measurements were performed on the 65- and 100-kGy irradiated UHMWPE (n=3 each) using a thermal mechanical analyzer (DMA 7e, Perkin Elmer, Wellesley, MA). Thin sections were machined out of the irradiated UHMWPE (3.2 mm thick) and were melted at 170°C under vacuum to remove residual stresses from the consolidation process that might result in dimensional changes during swelling. These thin sections were further cut into swelling test samples with a razor blade to approximately 3×3×3.2 mm. These were placed under the quartz probe of the TMA and the initial height, h_i, was recorded. Then, the probe and the test samples were immersed in xylene, which was heated to 130°C and held for at least 100 minutes until equilibrium swelling was reached. The final swollen height, h_f, of the test sample was recorded. The cross-link density was calculated using the swell ratio ($=hf^3/hi^3$) and Flory's theory of swollen networks as described previously [13] and reported as mol/m^3.

Doping in vitamin E

A 3 lt. round bottom reaction vessel with a four-neck top (6484, Ace Glass, Vineland, NJ) was filled with approximately 2 lt. of vitamin E (D,L-α-tocopherol, DSM Nutritional products, Belvidere, NJ). A stirrer blade (Fisher Maxima, Houston, TX) was fitted through the vessel neck for efficient stirring. A thermocouple was inserted through a rubber stopcock through the thermocouple fitting and the temperature was monitored as the vitamin E was placed in an air convection oven and heated to the desired temperature under continuous stirring. When the vitamin E equilibrated at the desired temperature, argon gas was connected to the assembly and a continuous argon purge was established. The temperature was allowed to equilibrate before samples were doped.

Cubes of unirradiated, 65- and 100-kGy irradiated UHMWPE (2×2×2 cm) were machined from the stock. Three cubes each were doped in vitamin E by soaking in the bath prepared as described above at 100°C, 110°C, 120°C, 130°C and 140°C for 24 hours. To determine the effect of time on the surface concentration, three cubes each were doped at 120°C for 2, 8 and 24 hours.

At the end of the doping time, the samples were taken out of the vitamin E bath and were allowed to cool to approximately room temperature. Subsequently, they were wiped with cotton gauze to remove excess vitamin E from the surface and the vitamin E concentration profiles were determined as described below.

Gravimetric changes as a result of doping were determined by weighing the cubes before doping and after doping, cooling down and wiping off the excess vitamin E and calculating the difference as a percentage of the initial weight. Volumetric change was determined by measuring each dimension of the cube at the midpoint with a micrometer, and calculating the difference as a percentage of the initial volume.

NIH-PA Author Manuscript

NIH-PA Author Manuscript

NIH-PA Author Manuscript

Determination of crystalline content

Thin sections (approximately 150 μm) were cut from doped UHMWPEs using a sledge microtome. Small specimens (~5–10 mg, n=3 each) for differential scanning calorimetry (DSC) were punched out near the edge of these thin sections that corresponded to one of the free surfaces of the doped UHMWPE and the vitamin E-free center. The DSC specimens were weighed on a Sartorius CP 225D balance to a resolution of 0.01 mg, placed in aluminum sample pans and the pans were crimped. The sample and reference were then heated in the DSC (Q1000, TA Instruments, Newark, DE) at 10°C/min from −20°C to 180°C. Heat flow as a function of time and temperature was recorded. Crystallinity was determined by integrating the heat flow curve from 20°C to 160°C, and normalizing to the enthalpy of melting of 100% crystalline polyethylene; 291 J/g.

Quantification of vitamin E concentration

Fourier Transform Infrared Spectroscopy (FTIR, Bio-Rad FTS155/UMA500, Natick MA) was performed on thin sections (approximately 150 μm) cut using a sledge microtome (Model 90-91-1177, LKB-Produkter AB, Bromma Sweden). Infrared spectra were collected from one edge of the sample to the other spanning two opposite free surfaces of the doped UHMWPE in 100 μm and 500 μm intervals, with each spectrum recorded as an average of 32 individual scans. The infrared spectra were analyzed to calculate a vitamin E index as the ratio of the areas under the α-tocopherol absorbance at 1262 cm^{-1} (1245–1275 cm^{-1}) and the polyethylene skeletal absorbance at 1895 cm^{-1} (1850–1985 cm^{-1}).

The penetration depth was defined as the depth from the free surface of the UHMWPE cube where the vitamin E index fell below 0.02, which is close to the Vitamin E detection limit of FTIR [21].

Analytic model of vitamin E doping

The diffusion coefficient, *D*, for vitamin E in UHMWPE was assumed to follow Arrhenian behavior with respect to temperature:

$$D = D_0 \cdot e^{-\frac{Q}{RT}} \quad \text{(Eq. 1)}$$

where D_0 is the diffusion constant, Q is the activation energy, R is the gas constant, and T is the temperature [24–27]. Diffusion constant is not dependent on time, hence one diffusion constant was calculated for each temperature.

The diffusion of vitamin E into UHMWPE during doping was assumed to follow Fick's second law of diffusion, where the concentration of vitamin E as a function of depth and time was:

$$C(x,\ t) = C_0 \cdot erfc\left(\frac{x}{2\sqrt{Dt}}\right) \quad \text{(Eq. 2)}$$

where C_0 is the saturation concentration of the material, x is depth, D is the diffusion coefficient, and t is time [24–27]. The complementary error function, *erfc(z)*, is simply [1−*erf(z)*]. The saturation concentration was assumed to be reached instantaneously and was obtained from the surface vitamin E concentration from the experimental data for doping at 24 hours.

An impedance factor, τβ, was calculated by dividing the diffusion coefficient of the amorphous polymer (140°C) by the diffusion coefficients below the melting point, where τ is the geometric impedance factor and β is the chain immobilization factor [28]. This is a measure of the impedance of crystallites on the diffusion of vitamin E in semi-crystalline UHMWPE.

NIH-PA Author Manuscript

NIH-PA Author Manuscript

NIH-PA Author Manuscript

Homogenization of vitamin E

Homogenization of the vitamin E profile subsequent to doping was done by placing the doped specimens in an empty reaction vessel at room temperature and heating them to the desired temperature under argon purge. At the end of the homogenization period, the samples were cooled down to approximately room temperature under argon flow.

Cubes of 65- and 100-kGy irradiated UHMWPE (2×2×2 cm) were machined from the stock. Three cubes each were doped in vitamin E as described above at 120°C for 2 hours. Subsequently, they were homogenized at 120°C for 24 hours. Three control samples were prepared by doping in vitamin E for 26 hours.

Analytical model of homogenization

Post-doping homogenization was modeled as a thin film of vitamin E diffusing into a semi-infinite UHMWPE medium (Fig 3). The concentration profile as a function of depth and time for a thin film of initial concentration C_0 and initial width $2h$ diffusing into an infinite medium was:

$$C(x,\ t) = \left(\frac{C_0}{2}\right) \cdot \left[erf\left(\frac{h - x}{2\sqrt{Dt}}\right) + erf\left(\frac{h + x}{2\sqrt{Dt}}\right)\right] \quad \text{(Eq. 3)}$$

where x is depth, D is the diffusion constant, and t is time [29,30]. Eq. 3 is valid for all depths in an infinite medium, $-\infty < x < +\infty$. The UHMWPE was modeled as a semi-infinite medium, thus only positive values of x were valid. Since vitamin E did not elute out of the material during homogenization, it can be assumed that there was an impermeable barrier at depth $x = 0$; therefore, by superposition, the concentration in Eq. 3 was multiplied by a factor of 2, giving:

$$C(x,\ t) = C_0 \cdot \left[erf\left(\frac{h - x}{2\sqrt{Dt}}\right) + erf\left(\frac{h + x}{2\sqrt{Dt}}\right)\right] \quad \text{(Eq. 4)}$$

The initial concentration C_0 was taken to be the same saturation limit C_0 calculated for doping. The width of the thin film was chosen such that the amount of vitamin E remained the same; that is, the area under the concentration profile after doping was equal to the area under the thin film, giving:

$$2h = \left(\frac{1}{C_0}\right) \cdot \int_0^\infty C(x,\ 0)dx \quad \text{(Eq. 5)}$$

The thin film width $2h$ for homogenization in Eq. 5 was calculated at homogenization time $t = 0$ at the conclusion of doping; homogenization time did not include and was not affected by doping time.

A goodness-of-fit test [31,32] was performed using χ^2 values for each sample set. Since the model had four independent variables, the χ^2 values were calculated and compared against the critical values for four degrees of freedom. If $\chi^2>9.49$, the probability that the predicted values matched the observed values was less than 5%, and the model would fail. If $\chi^2<0.71$, the probability that the predicted values matched observed values was greater than 95%, and the model could be said to predict the behavior well.

Sample groups were compared using a Student t-test where applicable. A p-value lower than 0.05 was considered significant.

NIH-PA Author Manuscript

NIH-PA Author Manuscript

NIH-PA Author Manuscript

Results and Discussion

Our aim was to study and model the diffusion of vitamin E in virgin UHMWPE and radiation cross-linked UHMWPE in order to predict diffusion profiles following doping of UHMWPE by soaking in vitamin E with subsequent homogenization at an elevated temperature. A Fickian model provided good fits with experimental data after soaking and after post soak homogenization.

In addition to the chemical interactions between UHMWPE and vitamin E, there are two structural features of semi-crystalline UHMWPE that will affect diffusion. The first is the crystalline lamellae and the second is the chemical cross-links formed in the amorphous phase of the polymer by irradiation. Unirradiated UHMWPE was used as a control in this study to differentiate the effects of the semi-crystalline nature of UHMWPE from the effects of cross-linking on the diffusion behavior of vitamin E.

A representative DSC trace of irradiated UHMWPEs taken from the vitamin E-rich surface and vitamin E-free bulk region of samples doped below the melting point (100°C) are shown in Figure 4. There was a single melting curve with a peak melting point of about 134°C for unirradiated (not shown) and 137–140°C for the irradiated UHMWPEs with no difference between vitamin E-rich and –free regions. The crystalline content of 65 and 100-kGy irradiated UHMWPEs was slightly higher than unirradiated UHMWPE in general (Table 1). The crystallinity of the vitamin E-rich region in the unirradiated UHMWPE was lower than that of 65-kGy and 100-kGy irradiated UHMWPE doped at 110 and 130°C ($p=0.01$, and 0.02 for 65-kGy and $p=0.02$ and 0.0005 for 100-kGy UHMWPE respectively). The crystallinity difference of the vitamin E-rich and vitamin E-free regions was only significant for unirradiated UHMWPE doped at 130°C and 140°C but that difference was small (Table 1, $p=0.01$).

Since the diffusion of vitamin E is reserved to the amorphous regions of the polymer, doping with vitamin E should have had no effect on the crystallinity of the UHMWPEs below the melting point. This was true for all conditions except unirradiated UHMWPE doped at 130° C. This was due to the fact that at doping temperatures close to the peak melting point of UHMWPE, more of the crystals were melting, thereby increasing the diffusion volume for vitamin E. However, it is possible that a large amount of vitamin E diffusion into these newly melted regions may prevent re-crystallization when cooled back to room temperature. This is more likely to happen in unirradiated UHMWPE due to the slightly lower melting temperature of this UHMWPE, causing more of the crystals to melt at 130°C than irradiated UHMWPEs and also due to the lack of cross-links to slow the diffusion of vitamin E.

Since unirradiated UHMWPE lacks chemical cross-links, once the polymer melts, it can easily be dissolved in a compatible solvent such as vitamin E. Solvation would then decrease overall crystallinity upon re-crystallization because the formation of crystals is not energetically favorable for chains still interacting with the solvent molecules. The significant crystallinity differences between the vitamin E-rich and vitamin E-free regions in all UHMWPEs doped at 130 and 140°C (Table 1) corroborated this explanation. For samples doped at 140°C, above the melting point, the crystallinity of unirradiated and irradiated UHMWPEs was not significantly different, but the crystallinity was significantly lower than that for samples doped at 100–130°C. Also, the crystallinity of the vitamin E-free region was significantly higher than that for the vitamin E-rich region for unirradiated UHMWPE doped above the melting point ($p=0.04$).

Below the melting point, crystallinity was not affected significantly by radiation cross-linking or vitamin E doping itself, but a major factor affecting the diffusion of vitamin E was expected to be cross-link density. The mechanical properties and wear of UHMWPE are significantly decreased as a function of increasing radiation dose [13,14] and overall cross-link density is

NIH-PA Author Manuscript

NIH-PA Author Manuscript

NIH-PA Author Manuscript

increased (Table 2, p=0.03). Hence, we hypothesized that the diffusion behavior of vitamin E would be different with increasing radiation dose. On the contrary, we found small differences between the surface vitamin E concentration, penetration depth and overall amount of diffused vitamin E for 65- and 100-kGy irradiated UHMWPEs doped below the melting point (Figures 5b and 5c, Table 3 and 4). All of these outcomes were lower for both of the irradiated UHMWPEs compared to unirradiated and uncross-linked UHMWPE (Table 5), suggesting that cross-linking to 65-kGy did affect diffusion, but the cross-link density differences between 65-and 100-kGy irradiation did not affect diffusion significantly.

There was a significant increase in the surface concentration of vitamin E in all UHMWPEs with increasing doping temperature from 100 to 130°C; below the melting point of UHMWPE (Fig 5a–c, $p<0.05$ for all). The amount of vitamin E that diffused into the UHMWPE was also significantly higher with increasing temperature ($p<0.05$ for all, Table 3–5). The surface concentration and the weight of diffused vitamin E was significantly higher for unirradiated UHMWPE than 65- and 100-kGy irradiated UHMWPE at all temperatures from 100–130°C except 100°C ($p<0.05$ for all except p=0.06 for 65-kGy and p=0.05 for 100-kGy at 100°C). The weight increase due to vitamin E was accompanied by a volumetric expansion, which increased with increasing temperature (Table 3–5). The penetration depth for unirradiated UHMWPE was higher than that for both of the irradiated UHMWPEs at each temperature. There were no differences in penetration depth between the 65- and 100-kGy irradiated UHMWPEs. Above the melting point of UHMWPE, at 140°C, there were no significant differences between the penetration depth of unirradiated UHMWPE and the two irradiated UHMWPEs ($p>0.05$) despite lower surface concentration for 65-kGy irradiated UHMWPE (Tables 3–5, Fig 6).

Increasing the doping temperature close to and above the peak melting point increased vitamin E diffusion in both unirradiated and irradiated UHMWPEs drastically (Figs 5a–c, Fig 6) presumably due to the large increase in amorphous content (percent melted in Fig 2) and also due to increased energy associated with increased temperature. Above the melting point of all UHMWPEs, differences between surface concentrations and penetration depth were similar, suggesting that the effect of the cross-links were made negligible by the increase in the amorphous content. This is also because the melted crystalline regions contain no cross-links, thereby introducing a relatively unhindered amorphous volume for diffusion. If UHMWPE had been irradiated in the melt phase, then the distribution of cross-links would have been more uniform and the effect of cross-links could perhaps be observed also in the melt-phase.

The surface vitamin E concentration of the unirradiated and irradiated UHMWPEs increased rapidly with doping time (Figs 7a–c). The surface concentration of vitamin E increased significantly at 8 hours doping compared to 2 hours doping for unirradiated and 100-kGy irradiated UHMWPE (p=0.01 and 0.04, respectively) and also at 24 hours doping compared to 8 hours doping for all samples doped at 120°C with increasing time (p=0.01, 0.005 and 0.03 for unirradiated, 65-kGy irradiated and 100-kGy irradiated UHMWPE, respectively; Figures 7a–c). The penetration depth increased significantly at 8 hour doping compared to 2 hour doping for all UHMWPEs (p=0.04 for unirradiated, p=0.004 for 65-kGy and p=0.0004 for 100-kGy irradiated UHMWPE), but it was significantly changed only for 65-kGy irradiated UHMWPE doped for 24 hours compared to 8 hours (p=0.01). The lower solubility for irradiated UHMWPEs (compared to unirradiated UHMWPE) despite similar crystalline content below 130°C suggested that cross-linking at or near the surface was instrumental in decreasing effective amorphous content for diffusion. This may have occurred due to the clustering of molecules at cross-links, which may have created regions with mesh sizes smaller than what is necessary for the vitamin E molecules to pass through, thereby making some amorphous content not effective for diffusion. Although there was a significant increase in the amount of diffused vitamin E with increasing temperature, the largest differential increase occurred from

NIH-PA Author Manuscript

NIH-PA Author Manuscript

NIH-PA Author Manuscript

120 to 130°C. At 130°C, after 24 hours of doping, vitamin E constituted about 10–15% of the irradiated UHMWPEs and about 45% of unirradiated UHMWPE (Fig 8, Table 3–5).

Vitamin E exhibited Fickian diffusion behavior in both unirradiated and irradiated UHMWPE with diffusion coefficients on the order of 10^{-5} to 10^{-6} mm^2/s (Fig 9–10). The calculated diffusion coefficients showed Arrhenian behavior as described by the high R^2 values of the calculated diffusion coefficients against 1/Temperature (Fig 10). The diffusion constants and activation energy describing the Arrhenian behavior for unirradiated UHMWPE were lower than that for the irradiated UHMWPEs. The diffusion constant and the activation energy for 65-kGy irradiated UHMWPE were also slightly lower than that for 100-kGy irradiated UHMWPE. The diffusion coefficients of unirradiated and irradiated UHMWPEs approached each other at 130°C (Fig 10, Table 6). Above the melt at 140°C, the diffusion coefficients were about two orders of magnitude higher than those below the melting point (Tables 6 and 7). The diffusion model was used for temperatures below the melting point of UHMWPE assuming insignificant changes in crystallinity. The value calculated at 140°C can be considered to be the diffusion coefficient of completely amorphous UHMWPE and the impedance of the crystals and the cross-links in the solid phase can be calculated from this value. The multiple of the geometric impedance factor, τ, and the chain immobilization factor, β, previously described for polyethylene, showed that impedance was similar for unirradiated and irradiated UHMWPEs and this impedance decreased as a function of increasing temperature. Therefore, the dependence of diffusion rate on cross-linking appeared not to be strong. Significances were not calculated due to the large standard deviation in the results. The impedance created by the crystallites and the cross-links decreased with increasing temperature (Table 7). The fit of the diffusion profiles using the diffusion coefficients obtained was very good with χ^2 values of 0.01 and 0.23 for 2 and 24 hour doping of unirradiated UHMWPE, 0.52 and 0.64 for 65-kGy irradiated UHMWPE and 0.19 and 0.45 for 100-kGy irradiated UHMWPE, respectively.

It is necessary to obtain vitamin E throughout joint implant components for oxidative stability. However, we wanted to obtain vitamin E throughout UHMWPE joint implants without morphological changes associated with high surface concentrations of vitamin E and without significant distortion of the components due to exposure to high temperature and large amounts of vitamin E. To achieve this goal, we restricted the diffusion to 120° C since we determined that significant volumetric and weight change were seen above this temperature (Fig 8a). We also used doping for a short duration to achieve a high surface concentration, which was then homogenized throughout the component by subsequent homogenization in inert gas. The vitamin E concentration profiles of 65-kGy and 100-kGy irradiated UHMWPE (1) doped at 120°C for 26 hours and (2) doped at 120°C for 2 hours, subsequently homogenized at 120°C for 24 hours are shown in Figures 11a and 11b. The penetration depth was similar in these two methods; however, the surface concentration and the diffused vitamin E amount for the doped and homogenized UHMWPE were significantly lower (Tables 8–9; p=0.0007 and p=0.0004, respectively). The weight change is also accompanied by a similar volumetric change (59% for 65-kGy and 109% for 100-kGy). We achieved our goal using this combination; both getting good penetration of vitamin E (Figs 11a and 11b) as well as minimal dimensional change (Tables 8 and 9).

We had hypothesized that the diffusion coefficients calculated from diffusion studies above could be used to describe further diffusion of the vitamin E in the homogenization step. The surface concentration values showed an exponential dependence on increasing temperature (Fig 12), which was incorporated into the Fickian model to describe the diffusion of the vitamin E on the surface into the bulk of a semi-infinite slab of UHMWPE during the homogenization process. The experimental vitamin E concentration profiles and those predicted by using the diffusion coefficients obtained from the model above are shown for doped and subsequently homogenized 65- and 100-kGy irradiated UHMWPE (Figs 13a and 13b). The fit of the model

NIH-PA Author Manuscript

NIH-PA Author Manuscript

NIH-PA Author Manuscript

was relatively good with χ^2 values on the order of 0.8. Our hypothesis tested positive; by using the Fickian diffusion model developed above, we were able to predict the vitamin E concentration profiles of 65- and 100-kGy irradiated, doped and homogenized UHMWPE doped for 2 hours followed by homogenization for 24 hours (Fig 13a and 13b). Such a method gave a penetration of about 3.5 mm, which would allow a joint implant component of 7 mm to be stabilized against oxidation using vitamin E.

One limitation of this study is that the model is only valid for the range of temperatures studied. As crystallinity changes significantly close to or above the melting point, the activation energy changes drastically. Thus the model presented here may only be valid up to 130°C. The doping and homogenization of irradiated UHMWPE components used in total joint arthroplasty would typically be carried out at above 100°C to accelerate the process and below the melt transition of UHMWPE to retain its mechanical properties. Therefore, the analytic model as presented here is valid for the temperature range in which vitamin E doping and homogenization would likely be carried out.

A second limitation is short duration (less than one hour) doping and homogenization. In developing the model we assumed that the surface vitamin E concentration instantaneously rises to C_0 (Fig 12) and slowly diffuses inwards – this would happen in a more idealized situation, such as gas molecules diffusing into a crystal lattice. Furthermore, durations less than one hour do not guarantee temperature uniformity throughout a UHMWPE sample, which would also affect diffusion. The model also idealizes the vitamin E concentration profile as a simple block at the start of homogenization instead of the true concentration profile after doping (Fig 3). Thus, the concentration profiles may not match after very short homogenization times.

Conclusion

The diffusion behavior of irradiated UHMWPE was different from unirradiated UHMWPE due to lower surface concentration, higher diffusion constant and higher activation energy although radiation dose did not have a large effect on these factors for 65- and 100-kGy. By using a Fickian model, we were able to describe the diffusion behavior and predict vitamin E concentration profiles for vitamin E-doped samples. Further, we developed a method to penetrate vitamin E in UHMWPE joint components by doping in vitamin E followed by homogenization in inert gas below the melting point of the polymer, thereby reducing the surface concentration and minimizing the morphological and dimensional effects of high vitamin E concentrations on UHMWPE. We were able to predict homogenized profiles relatively well using the Fickian model. The method and the model described here can potentially be used to penetrate and model the diffusion of other small molecular weight molecules in polyolefins or semi-crystalline polymers.

Acknowledgements

This study was funded by NIH R01 AR051142.

References

1. Muratoglu, OK.; Kurtz, S. Alternate Bearing Surfaces in Hip Replacement. In: Sinha, R., editor. Hip Replacement. Current Trends and Controversies; New York, NY: 2002. p. 1-46.
2. Kurtz SM, Rimnac CM, Pruitt L, Jewett CW, Goldberg V, Edidin AA. The relationship between the clinical performance and large deformation mechanical behavior of retrieved UHMWPE tibial inserts. Biomaterials 2000;21:283–291. [PubMed: 10646945]
3. Edidin AA, Pruitt L, Jewett CW, Crane DJ, Roberts D, Kurtz SM. Plasticity-induced damage layer is a precursor to wear in radiation-cross-linked UHMWPE acetabular components for total hip

NIH-PA Author Manuscript

NIH-PA Author Manuscript

NIH-PA Author Manuscript

replacement. Ultra-high-molecular-weight polyethylene. Journal of Arthroplasty 1999;14(5):616–27. [PubMed: 10475563]

4. Willert H, Bertram H, Buchhorn G. Osteolysis in alloarthroplasty of the hip. The role of bone cement fragmentation. Clin Orthop 1990;258:108–121. [PubMed: 2203567]
5. Willert HG, Bertram H, Buchhorn GH. Osteolysis in alloarthroplasty of the hip: The role of ultra-high molecular weight polyethylene wear particles. Clin Orthop 1990;258:95–107. [PubMed: 2203577]
6. Grobbelaar CJ, DuPlessis TA, Marais F. The Radiation Improvement of Polyethylene Prostheses. J Bone and Joint Surg 1978;60-B(3):370–374.
7. Muratoglu, O.; Bragdon, D.; O'Connor, D.; Jasty, M.; Harris, W. A novel method of crosslinking UHMWPE to improve wear with little or no sacrifice of mechanical properties. Society for Biomaterials 25th Annual Meeting Transactions; 1999; Providence, RI. 1999. p. 496
8. McKellop, H.; Shen, F-W.; Salovey, R. Extremely low wear of gamma-crosslinked/remelted UHMWPE acetabular cups. Proceedings of ORS; 1998. p. 98
9. Nivbrant, B.; Roerhl, S.; Hewitt, B.; Li, M. In vivo wear and migration of high cross linked poly cups: A RSA study. 49th Annual Orthopaedic Research Society; 2003; New Orleans, LA. 2003. p. 358
10. Digas G, Karrholm J, Thanner J, Malchau H, Herberts P. Highly cross-linked polyethylene in total hip arthroplasty: randomized evaluation of penetration rate in cemented and uncemented sockets using radiostereometric analysis. Clin Orthop 2004;(429):16.
11. Kawakage NOS, Ogihara T. Poly (vinyl alcohol)-clay and poly (ethylene oxide)-clay blends prepared using water as solvent. J Applied Polymer Science 1997;66:573–581.
12. Sutula L, Collier J, Saum K, Currier B, Currier J, Sanford W, et al. The Otto Aufranc Award. Impact of gamma sterilization on clinical performance of polyethylene in the hip. Clin Orthop 1995;(319): 28–40. [PubMed: 7554641]
13. Muratoglu OK, Bragdon CR, O'Connor DO, Jasty M, Harris WH, Gul R, et al. Unified Wear Model for Highly Crosslinked Ultra-high Molecular Weight Polyethylenes (UHMWPE). Biomaterials 1999;20(16):1463–1470. [PubMed: 10458559]
14. Oral E, Malhi A, Muratoglu O. Mechanisms of decrease in fatigue crack propagation resistance in irradiated and melted UHMWPE. Biomaterials 2006;27:917–925. [PubMed: 16105682]
15. Oral E, Wannomae KK, Hawkins NE, Harris WH, Muratoglu OK. α-Tocopherol Doped Irradiated UHMWPE for High Fatigue Resistance and Low Wear. Biomaterials 2004;25(24):5515–5522. [PubMed: 15142733]
16. Oral E, Wannomae K, Huang A, Rowell S, Muratoglu O. α-Tocopherol diffusion into UHMWPE. I. Diffusion and homogenization in highly cross-linked UHMWPE. Polymer. 2006submitted
17. Oral E, Christensen S, Malhi A, Wannomae K, Muratoglu O. Wear resistance and mechanical properties of highly crosslinked UHMWPE doped with vitamin E. Journal of Arthroplasty 2006;21 (4):580–591. [PubMed: 16781413]
18. Packer L. Protective role of vitamin E in biological systems. Am J Clin Nutr 1991;53:1050S–1055S. [PubMed: 2012017]
19. Packer, L.; Kagan, VE. Vitamin E: The antioxidant harvesting center of membranes and lipoproteins. In: Packer, L.; Fuchs, J., editors. Vitamin E in Health and Disease. New York: Marcel Dekker, Inc; 1993. p. 179-192.
20. Parth M, Aust N, Lederer K. Studies on the effect of electron beam radiation on the molecular structure of ultra-high molecular weight polyethylene under the influence of alpha-tocopherol with respect to its application in medical implants. J Mater Sci-Mater Med 2002;13(10):917–921. [PubMed: 15348184]
21. Oral E, Greenbaum E, Malhi A, Muratoglu O. Characterization of blends of α-Tocopherol with UHMWPE. Biomaterials 2005;26:6657–6663. [PubMed: 15993487]
22. Oral, E.; Wannomae, K.; Muratoglu, O. The effect of doping conditions on α-tocopherol stabilized UHMWPE. Transactions, 51st Annual Meeting of the Orthopaedic Research Society; 2005; Washington, D.C.. 2005.
23. Wolf C, Maninger J, Lederer K, Fruhwirth-Smounig H, Gamse T, Marr R. Stabilisation of crosslinked ultra-high molecular weight polyethylene (UHMW-PE)-acetabular components with alpha-tocopherol. J Mater Sci Mater Med 2006;17:1323–1331. [PubMed: 17143764]

NIH-PA Author Manuscript

NIH-PA Author Manuscript

NIH-PA Author Manuscript

24. Balluffi, RW.; Allen, SM.; Carter, WC. Kinetics of Materials. New York: John Wiley & Sons, Inc; 2003.
25. Poirier, DR.; Geiger, GH. Transport Phenomena in Materials Processing. Warrendale: The Minerals, Metals, & Materials Society; 1994.
26. Balluffi, R.; Allen, S.; Carter, W. Kinetics of Materials. New York: John Wiley&Sons, Inc; 2003.
27. Poirier, D.; Geiger, G. Transport Phenomena in Materials Processing. Warrendale: The Minerals, Metals & Materials Society; 1994.
28. Vieth, WR. Diffusion In and Through Polymers. New York: Oxford University Press; 1991.
29. Chiang, Y-M.; Birnie, D., III; Kingery, WD. Physical Ceramics: Principles for Ceramic Science and Engineering. New York: John Wiley & Sons, Inc; 1997.
30. Chiang, Y-M.; Birnie, DI.; Kingery, W. Physical Ceramics: Prinicples for Ceramic Science and Engineering. New York: John Wiley & Sons, Inc; 1997.
31. Snedecor, GW.; Cochran, WG. Statistical Methods. 8. Ames: Iowa State University Press; 1989.
32. Snedecor, G.; Cochran, W. Statistical Methods. Ames: Iowa State University Press; 1989.

NIH-PA Author Manuscript

NIH-PA Author Manuscript

NIH-PA Author Manuscript

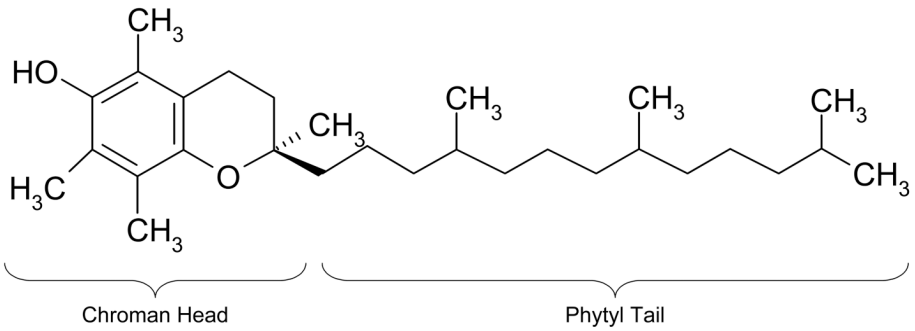

Fig 1.

α-Tocopherol. The chroman head is responsible for abstracting free radicals and stabilizing them within the structure. The long lipophilic ‘phytyl tail’ provides compatibility with UHMWPE.

NIH-PA Author Manuscript
NIH-PA Author Manuscript
NIH-PA Author Manuscript

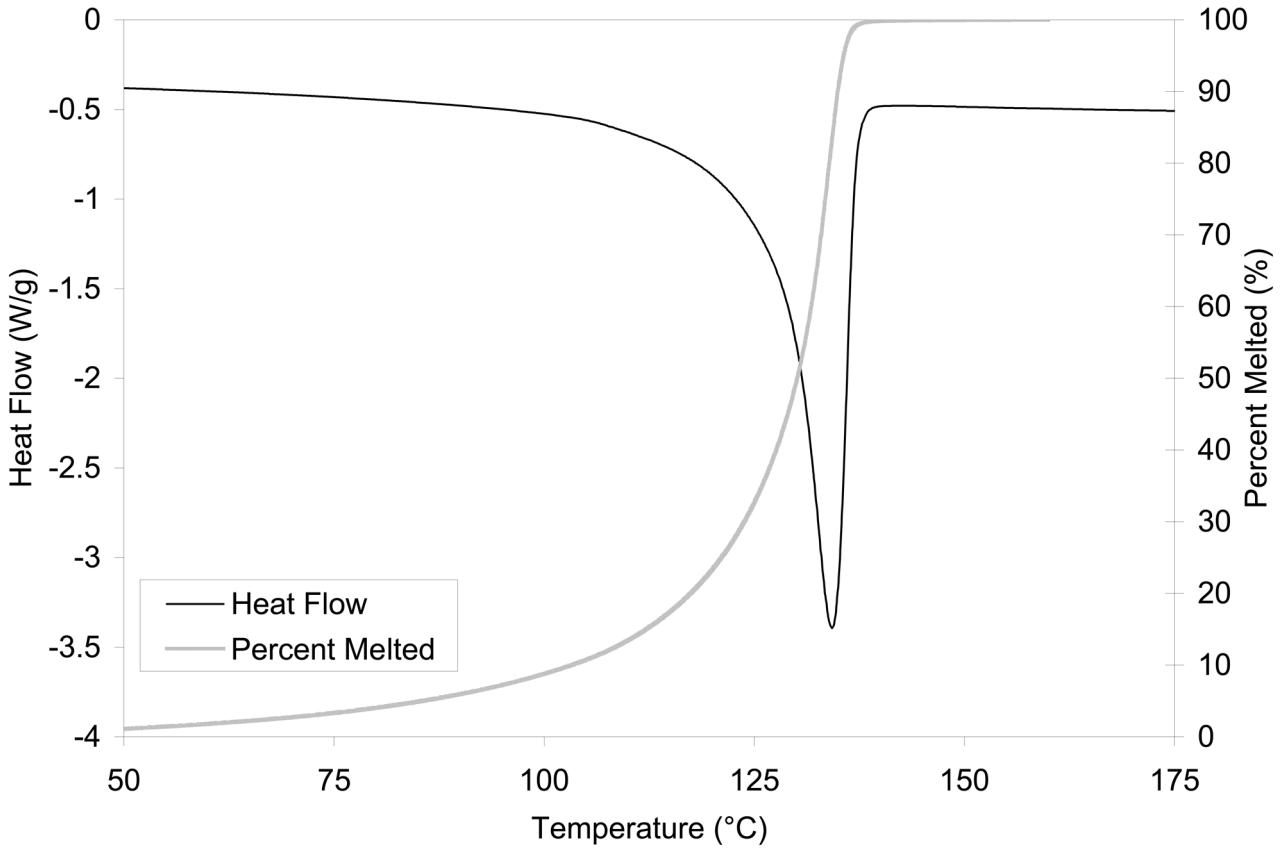

Fig 2.
A representative DSC thermogram of GUR1050 UHMWPE. Also plotted is the melted crystalline content as a function of temperature.

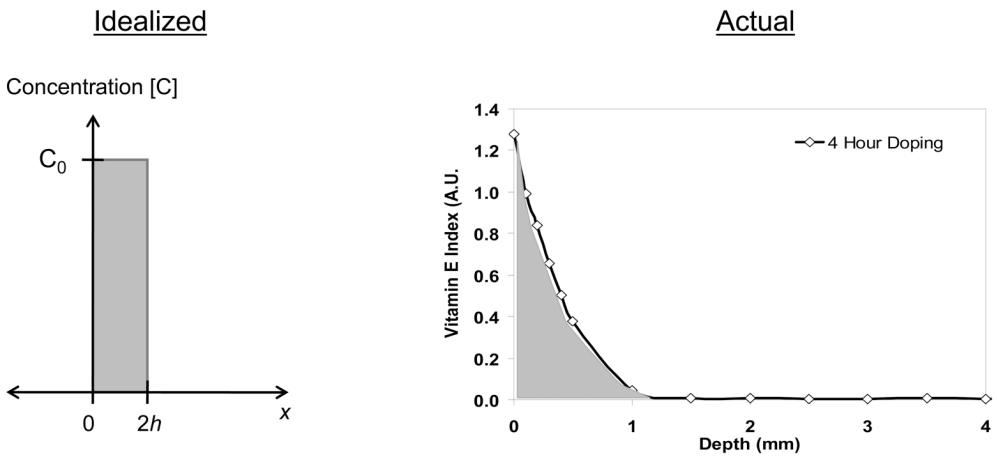

Fig 3.
Depiction of the assumed idealized concentration profile at the beginning of homogenization.

NIH-PA Author Manuscript
NIH-PA Author Manuscript
NIH-PA Author Manuscript

NIH-PA Author Manuscript

NIH-PA Author Manuscript

NIH-PA Author Manuscript

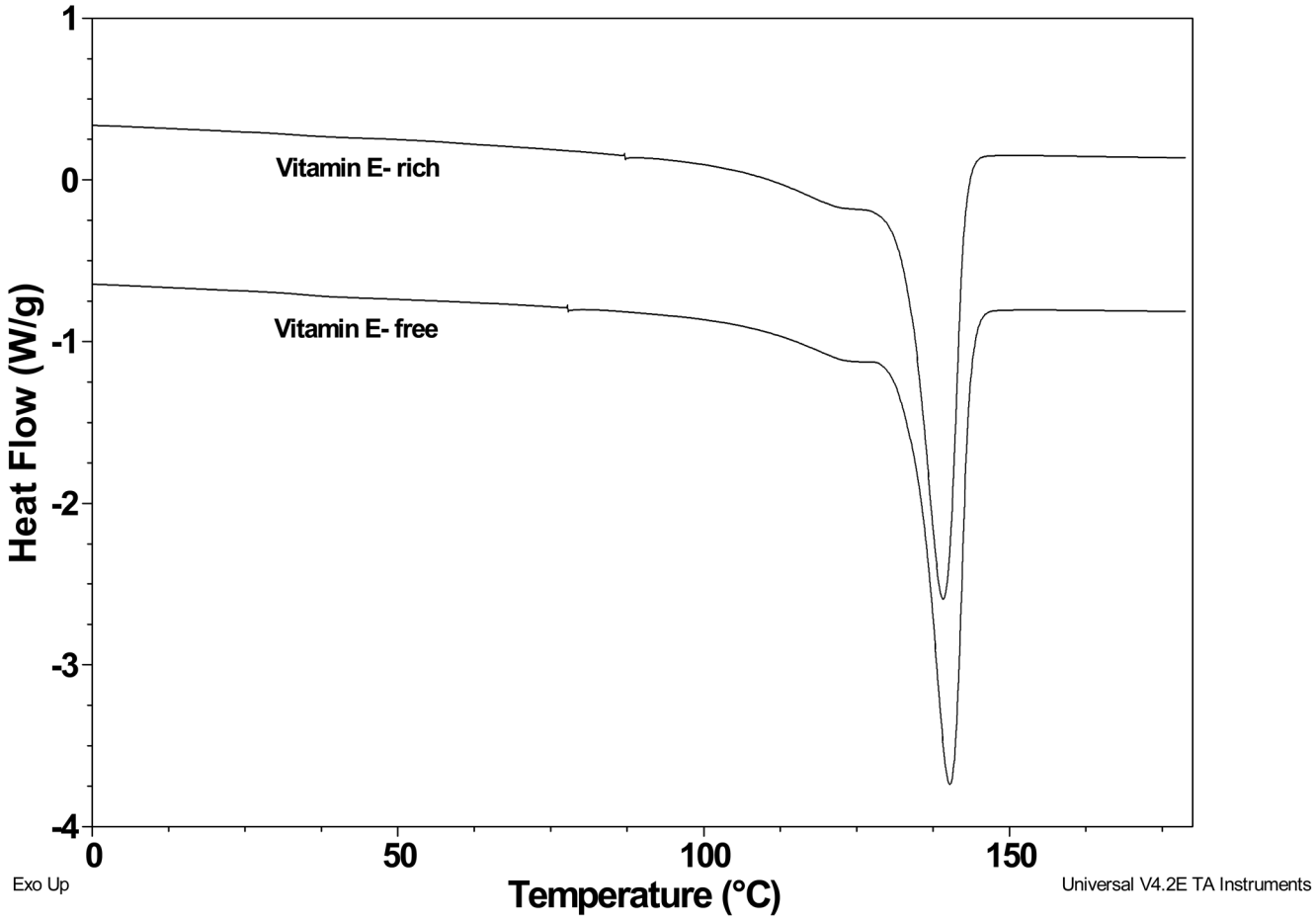

Fig 4.

Heat flow curves of vitamin E-doped 100-kGy irradiated UHMWPE from the vitamin E-rich surface region and the vitamin E-free bulk. Note that there was no difference in peak melting point and crystallinity between vitamin E-rich and vitamin E-free regions.

NIH-PA Author Manuscript

NIH-PA Author Manuscript

NIH-PA Author Manuscript

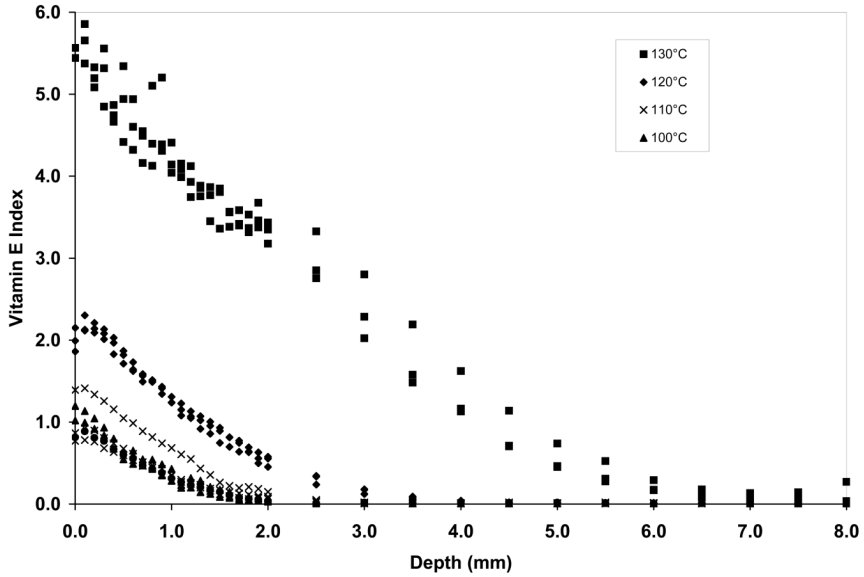

Fig 5a. Vitamin E concentration profiles of unirradiated UHMWPE doped with vitamin E for 24 hours as a function of temperature.

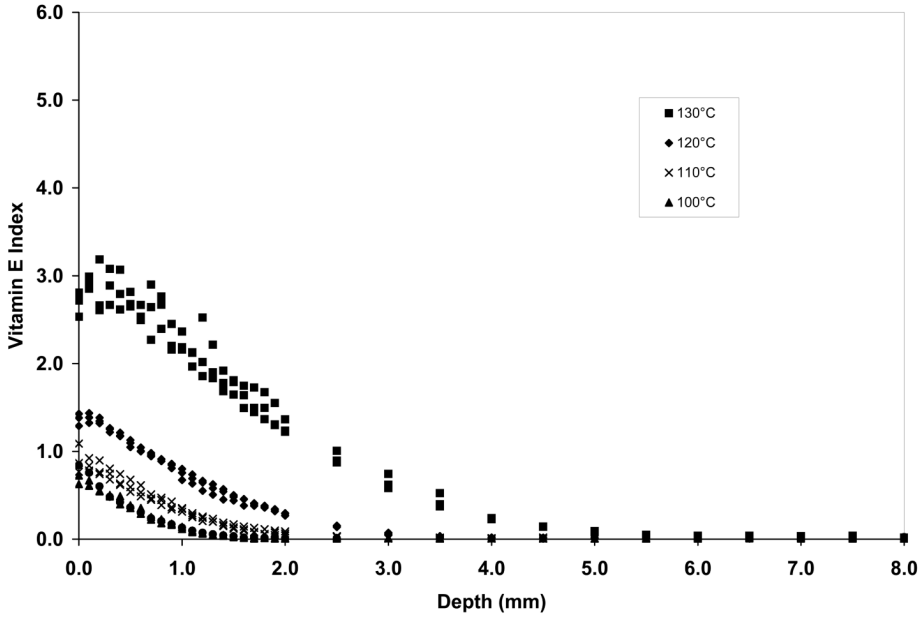

Fig 5b. Vitamin E concentration profiles of 65-kGy irradiated UHMWPE doped with vitamin E for 24 hours as a function of temperature.

NIH-PA Author Manuscript

NIH-PA Author Manuscript

NIH-PA Author Manuscript

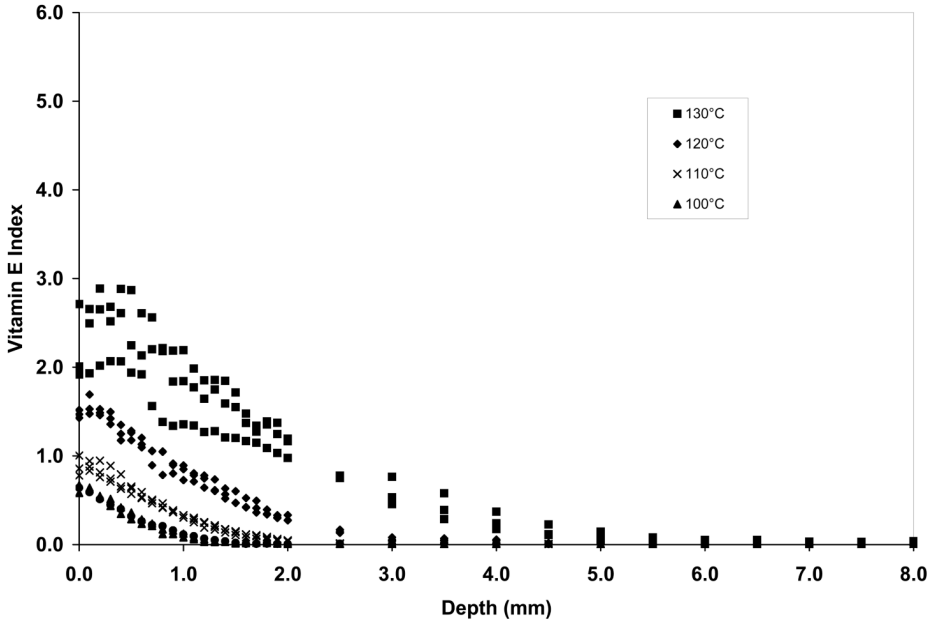

Fig 5c. Vitamin E concentration profiles of 100-kGy irradiated UHMWPE doped with vitamin E for 24 hours as a function of temperature.

Fig 5.

Vitamin E concentration profiles of unirradiated (a), 65-kGy irradiated (b) and 100-kGy irradiated (c) UHMWPE doped with vitamin E for 24 hours as a function of temperature.

NIH-PA Author Manuscript

NIH-PA Author Manuscript

NIH-PA Author Manuscript

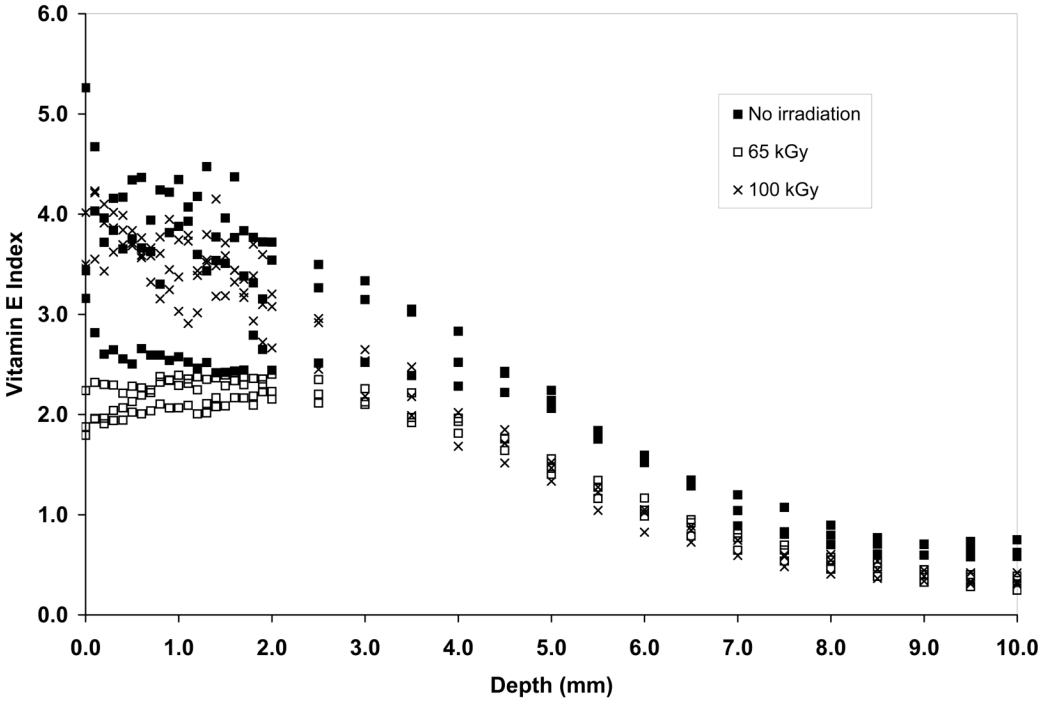

Fig 6.
Vitamin E concentration profiles of unirradiated, 65- and 100-kGy irradiated UHMWPE doped with vitamin E for 24 hours at 140°C.

NIH-PA Author Manuscript

NIH-PA Author Manuscript

NIH-PA Author Manuscript

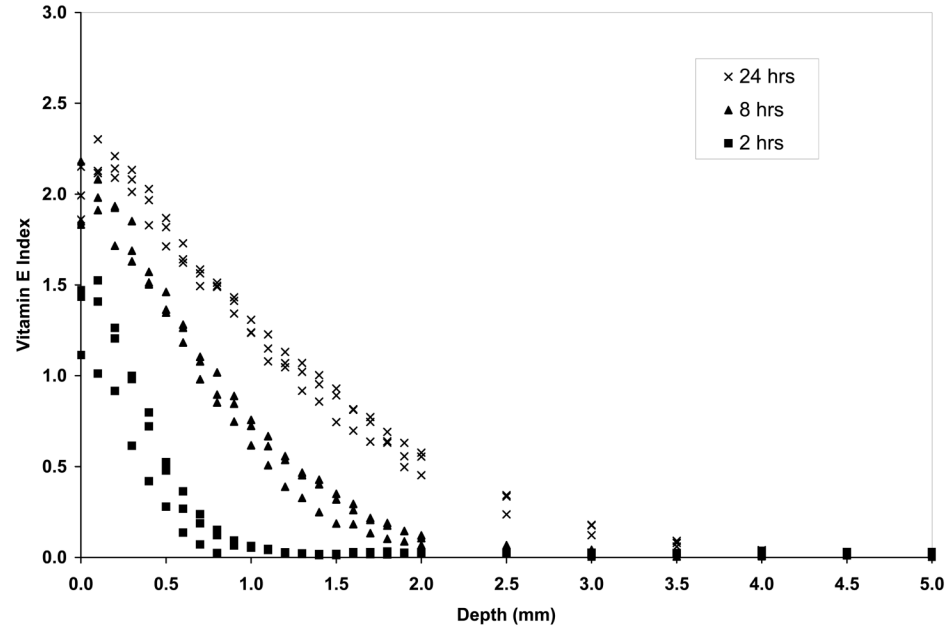

Fig 7a. Vitamin E concentration of unirradiated UHMWPE doped at 120°C as a function of time.

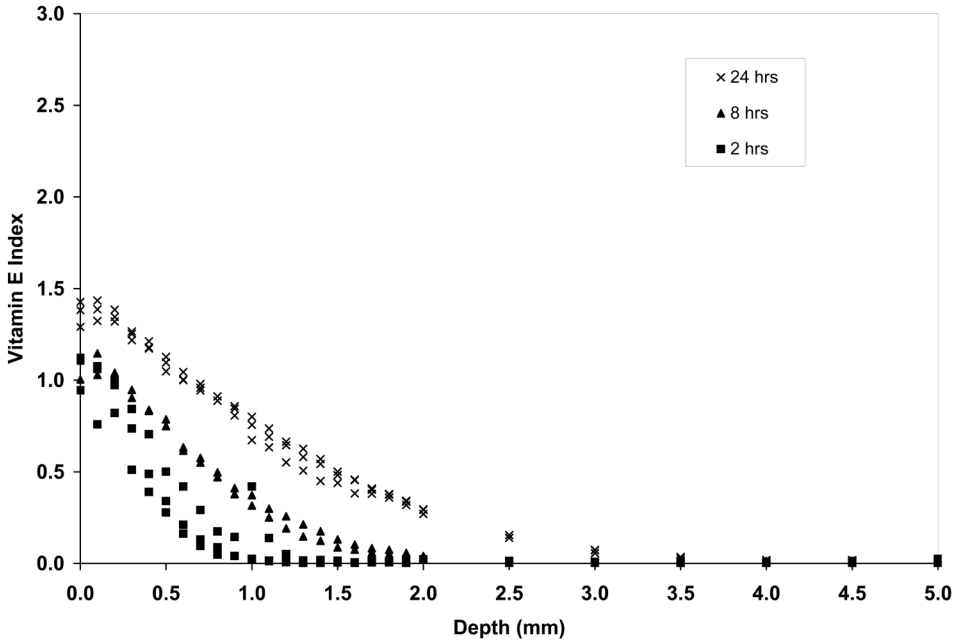

Fig 7b. Vitamin E concentration of 65-kGy irradiated UHMWPE doped at 120°C as a function of time.

NIH-PA Author Manuscript

NIH-PA Author Manuscript

NIH-PA Author Manuscript

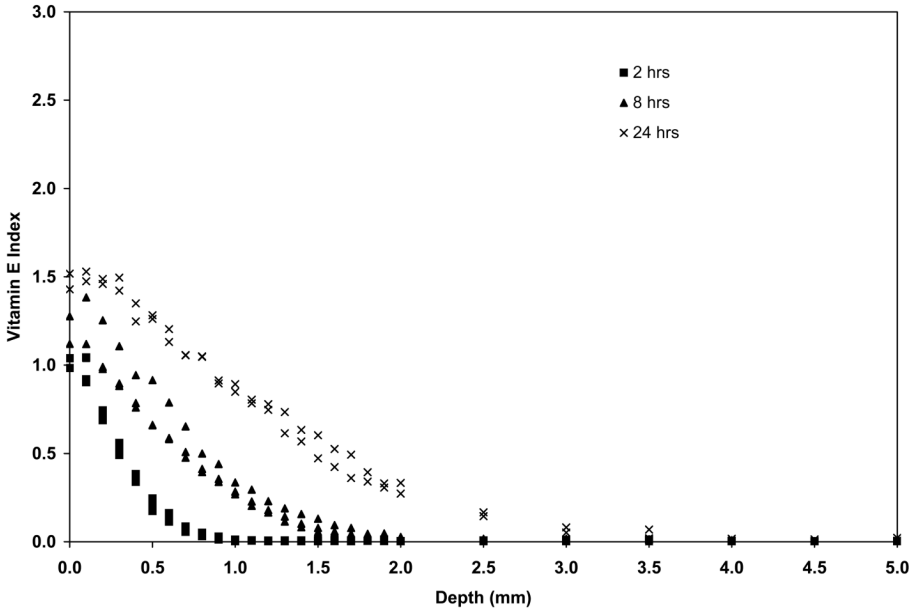

Fig 7c. Vitamin E concentration of 100-kGy irradiated UHMWPE doped at 120°C as a function of time.

Fig 7.

Vitamin E concentration of unirradiated (a), 65-kGy irradiated (b) and 100-kGy irradiated (c) UHMWPE doped at 120°C as a function of time.

NIH-PA Author Manuscript

NIH-PA Author Manuscript

NIH-PA Author Manuscript

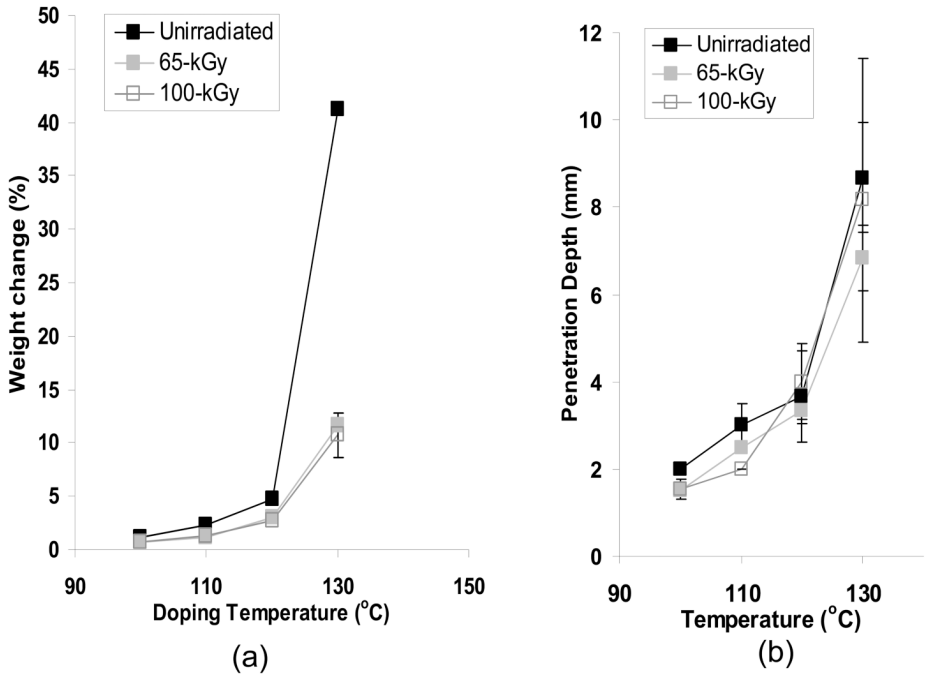

Fig 8.

Weight change as a result of vitamin E diffusion (a) and penetration depth of vitamin E in UHMWPE (b) as a function of doping temperature for samples doped for 24 hours.

NIH-PA Author Manuscript

NIH-PA Author Manuscript

NIH-PA Author Manuscript

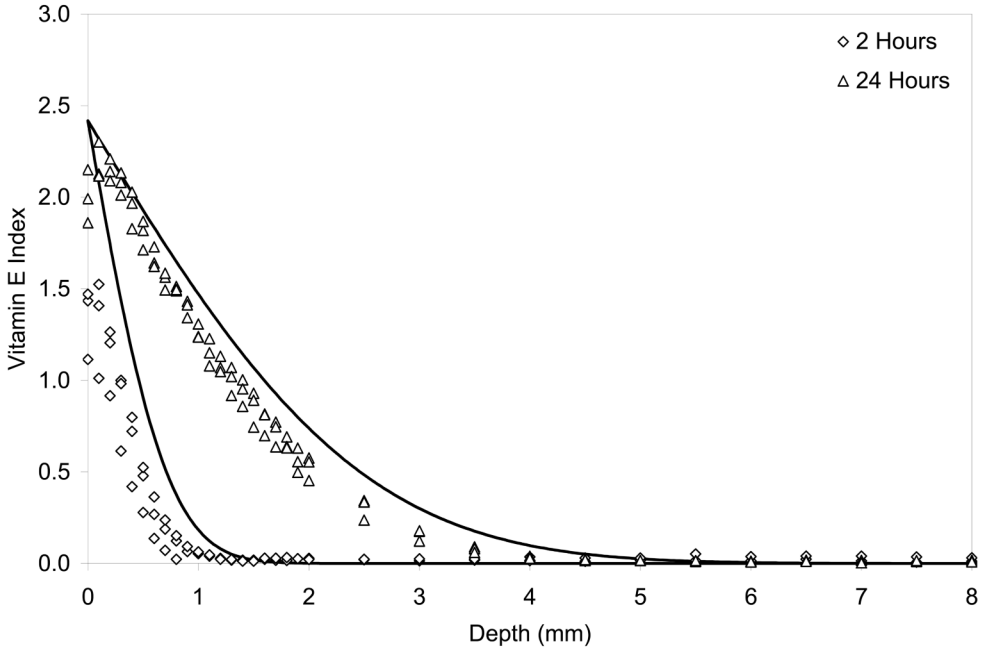

Fig 9a. Vitamin E concentration profiles of unirradiated UHMWPE doped at 120°C for 2 and 24 hours. The vitamin E profiles measured via FTIR (*n*=3 samples) are shown as individual data points; the predicted vitamin E concentration profile using Eqs. 2 and 3 is shown as the solid line.

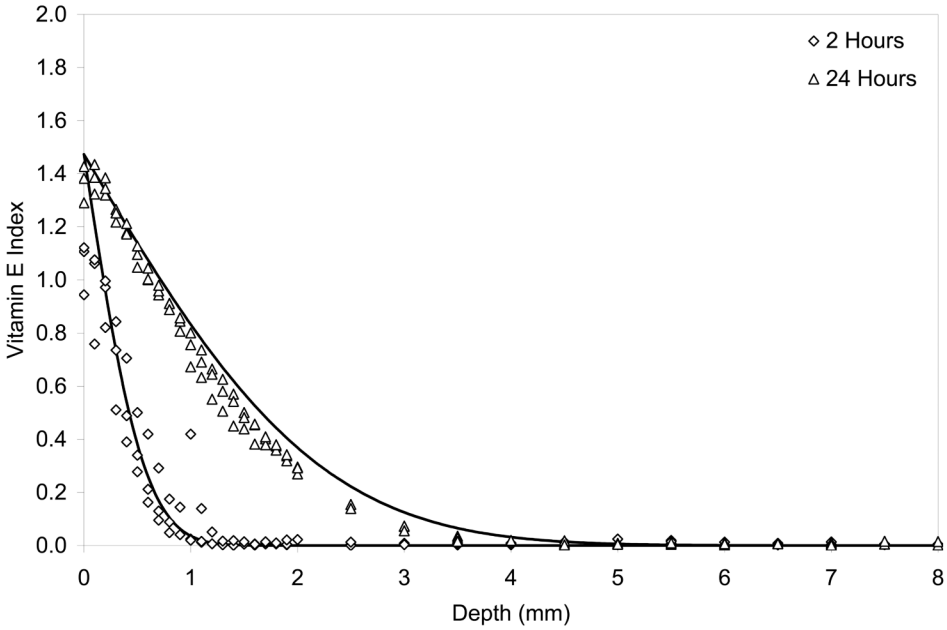

Fig 9b. Vitamin E concentration profiles of 65 kGy irradiated UHMWPE doped at 120°C for 2 and 24 hours. The vitamin E profiles measured via FTIR (*n*=3 samples) are shown as individual data points; the predicted vitamin E concentration profile using Eqs. 2 and 3 is shown as the solid line.

NIH-PA Author Manuscript

NIH-PA Author Manuscript

NIH-PA Author Manuscript

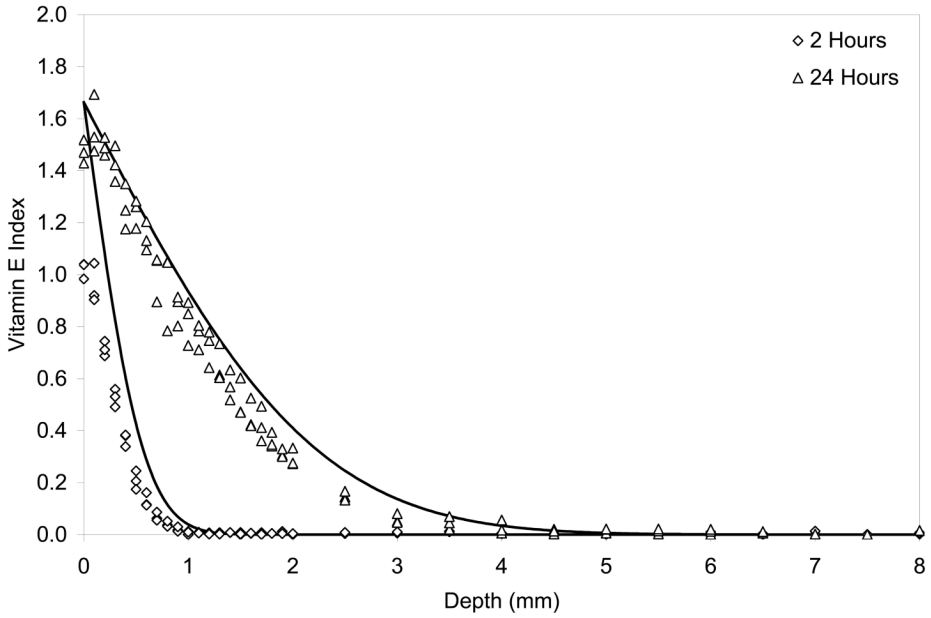

Fig 9c. Vitamin E concentration profiles of 100-kGy irradiated UHMWPE doped at 120°C for 2 and 24 hours. The vitamin E profiles measured via FTIR (*n*=3 samples) are shown as individual data points; the predicted vitamin E concentration profile using Eqs. 2 and 3 is shown as the solid line.

Fig 9.

Vitamin E concentration profiles of unirradiated (a), 65-kGy irradiated (b) and 100-kGy irradiated (c) UHMWPE doped at 120°C for 2 and 24 hours. The vitamin E profiles measured via FTIR (*n*=3 samples) are shown as individual data points; the predicted vitamin E concentration profile using Eqs. 2 and 3 is shown as the solid line.

NIH-PA Author Manuscript

NIH-PA Author Manuscript

NIH-PA Author Manuscript

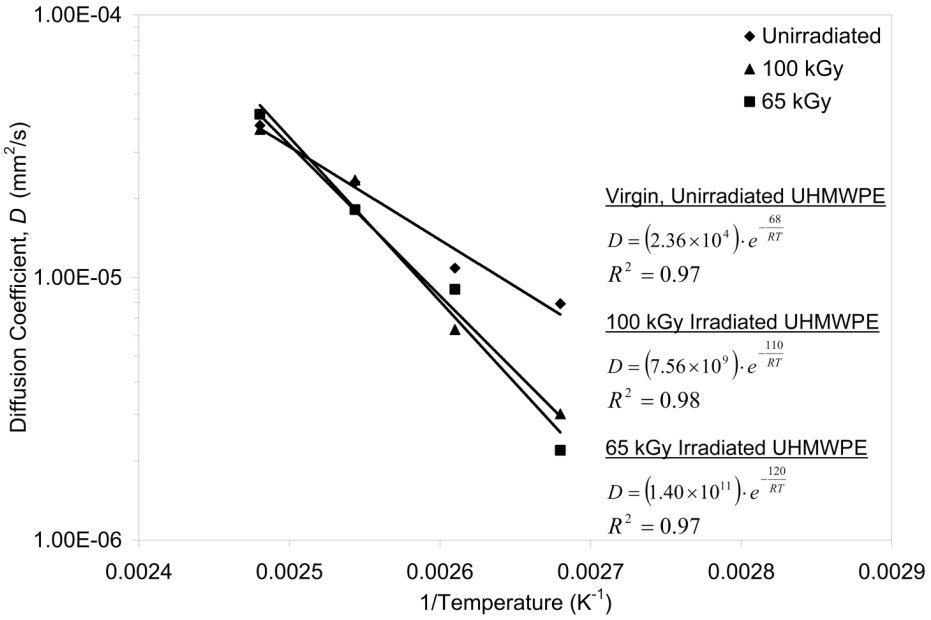

Fig 10.

Diffusion coefficient, *D*, as a function of 1/T (K^{-1}) for α-tocopherol into virgin, unirradiated UHMWPE and irradiated UHMWPE. The best fit exponential lines are shown, along with their equations and R^2 values. Average values of the diffusion coefficients were plotted without error bars for clarity.

NIH-PA Author Manuscript
NIH-PA Author Manuscript
NIH-PA Author Manuscript

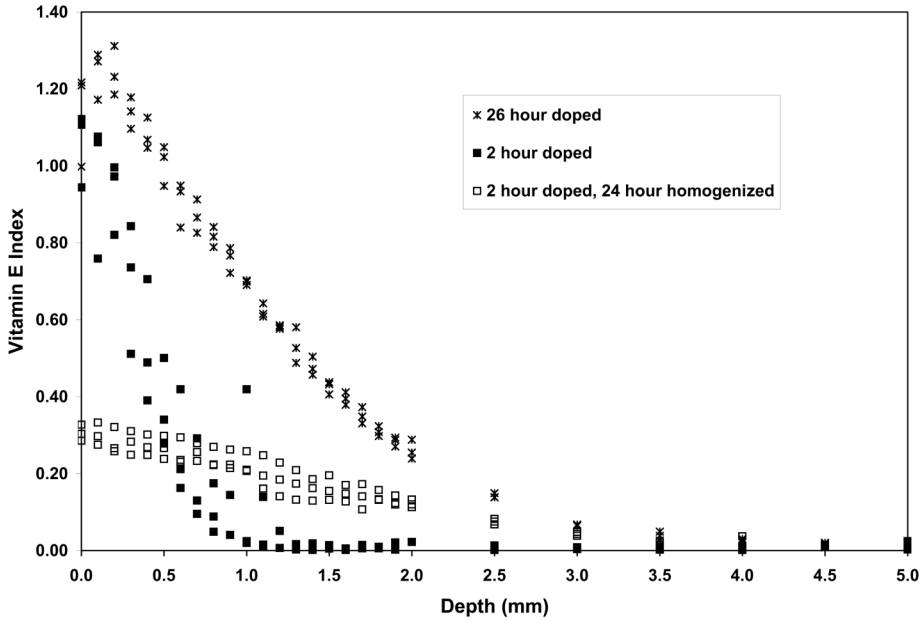

Fig 11a. Vitamin E concentration of 65-kGy irradiated UHMWPE doped at 120°C for 2 hours and homogenized for 24 hours compared to UHMWPE doped at 120°C for 26 hours.

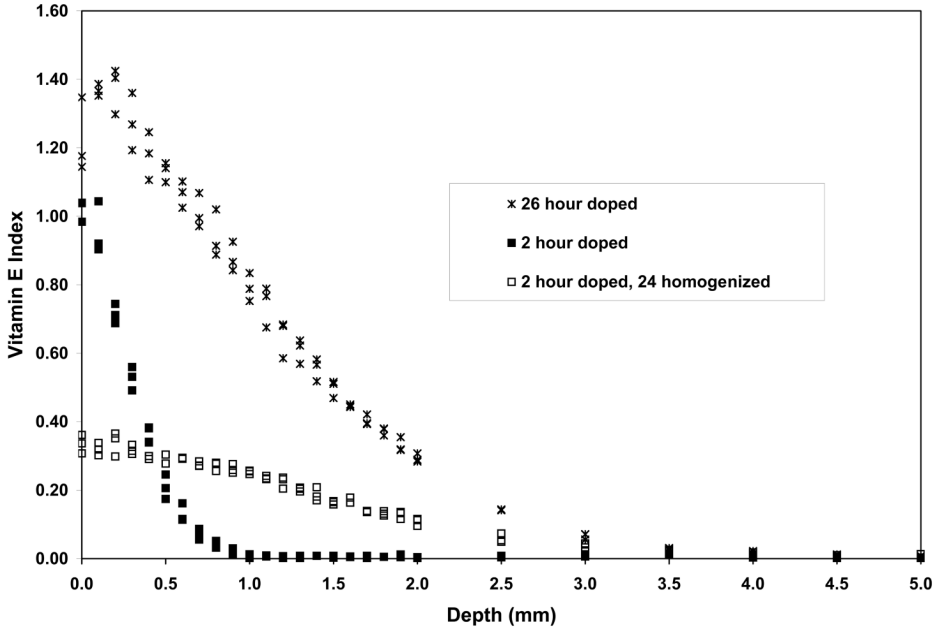

Fig 11b. Vitamin E concentration of 100-kGy irradiated UHMWPE doped at 120°C for 2 hours and homogenized for 24 hours compared to UHMWPE doped at 120°C for 26 hours.

Fig 11.

Vitamin E concentration of 65-kGy (a) and 100-kGy (b) irradiated UHMWPE doped at 120° C for 2 hours and homogenized for 24 hours compared to UHMWPE doped at 120°C for 26 hours.

NIH-PA Author Manuscript

NIH-PA Author Manuscript

NIH-PA Author Manuscript

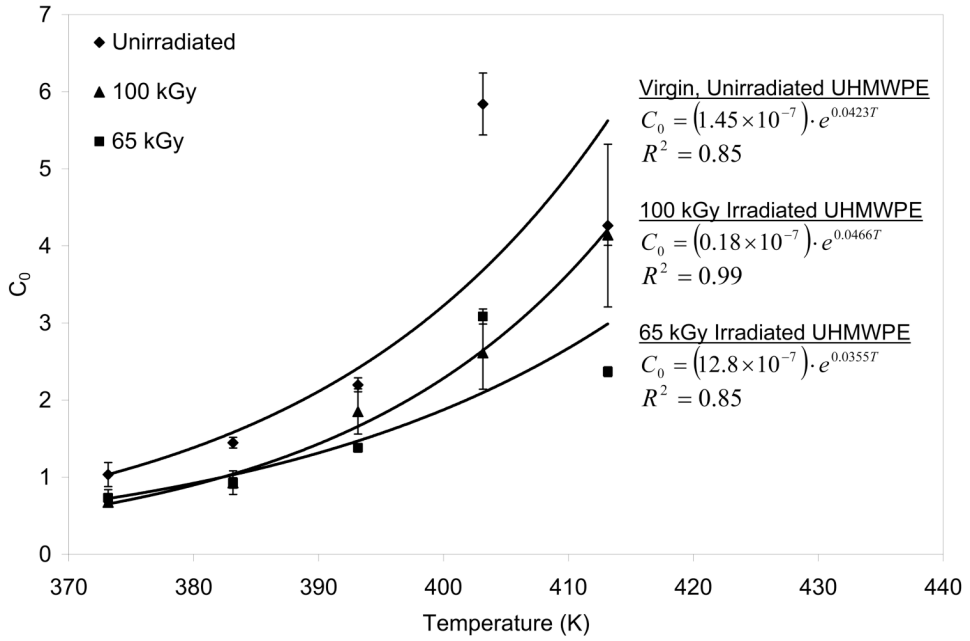

Fig 12.

Vitamin E saturation limit, C_0, as a function of T (K) for vitamin E into virgin, unirradiated UHMWPE and irradiated UHMWPE. The best fit exponential lines are shown, along with their equations and R2 values.

NIH-PA Author Manuscript

NIH-PA Author Manuscript

NIH-PA Author Manuscript

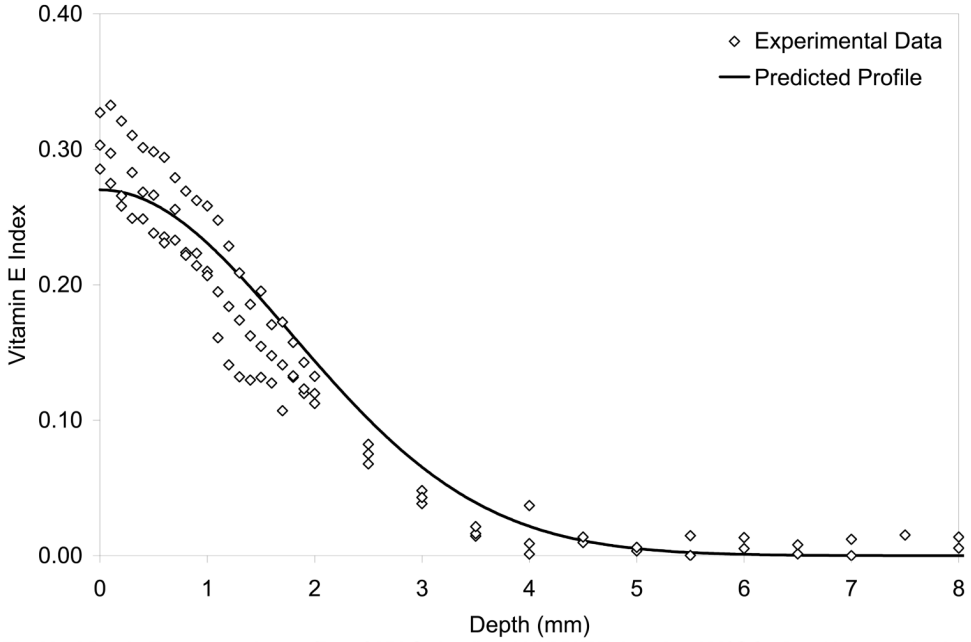

Fig 13a. Vitamin E concentration profiles of 65 kGy irradiated UHMWPE doped at 120°C for 2 and homogenized at 120°C for 24 hours. The vitamin E profiles measured via FTIR (*n*=3 samples) are shown as individual data points; the predicted vitamin E concentration profile using Eqs. 2 and 3 is shown as the solid line.

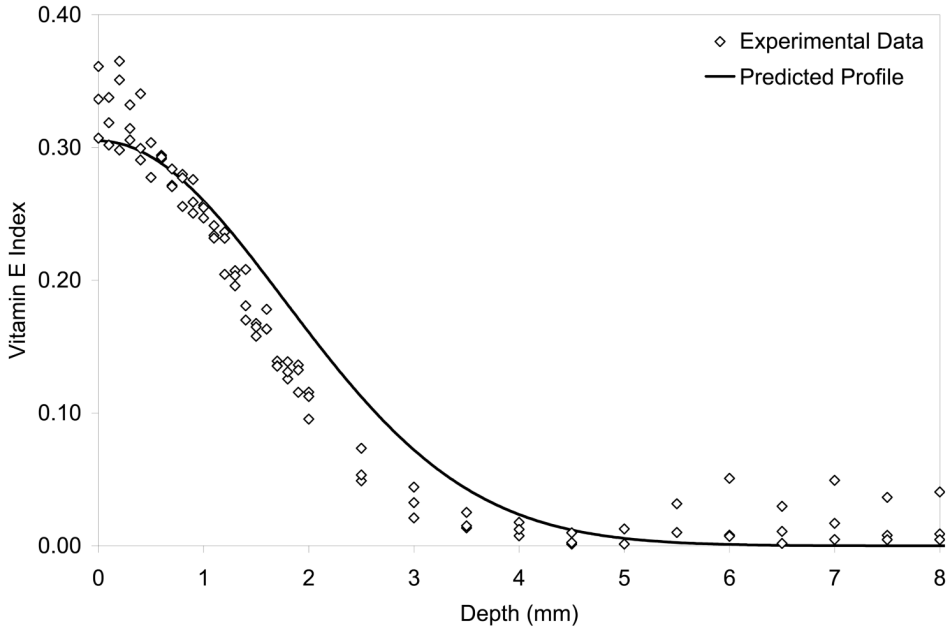

Fig 13b. Vitamin E concentration profiles of 100 kGy irradiated UHMWPE doped at 120°C for 2 and homogenized at 120°C for 24 hours. The vitamin E profiles measured via FTIR (*n*=3 samples) are shown as individual data points; the predicted vitamin E concentration profile using Eqs. 2 and 3 is shown as the solid line.

Fig 13.

Vitamin E concentration profiles of 65 kGy (a) and 100-kGy irradiated UHMWPE doped at 120°C for 2 and homogenized at 120°C for 24 hours. The vitamin E profiles measured via FTIR (*n*=3 samples) are shown as individual data points; the predicted vitamin E concentration profile using Eqs. 2 and 3 is shown as the solid line.

NIH-PA Author Manuscript
NIH-PA Author Manuscript
NIH-PA Author Manuscript

Table 1

Crystallinity (as determined by DSC) of unirradiated, 65- and 100-kGy irradiated UHMWPE from the surface vitamin E-doped regions and the bulk containing no vitamin E

Doping temperature	Unirradiated		65-kGy		100-kGy	
	Vitamin E	No Vitamin E	Vitamin E	No Vitamin E	Vitamin E	No Vitamin E
100°C	63.1±0.7	61.5±2.1	66.4±3.9	65.4±2.6	66.8±2.4	67.9±1.1
110°C	59.9±1.4	61.5±0.6	65.7±0.6	69.2±1.5	67.5±2.4	65.9±2.3
120°C	57.8±3.6	61.1±1.3	63.0±2.3	64.6±2.2	64.1±5.5	67.2±0.7
130°C	52.1±0.4	61.0±2.0	62.7±2.8	66.4±1.0	63.3±0.9	65.1±2.6
140°C	47.2±0.7	56.3±1.8	48.8±0.8	54.8±4.0	45.8±11.1	49.0±9.6

NIH-PA Author Manuscript
NIH-PA Author Manuscript
NIH-PA Author Manuscript

Table 2

Cross-link density of UHMWPE.

Temperature (°C)	Unirradiated	65-kGy	100-kGy
Cross-link density (mol/m^3)	NA	132±25	182±12

NIH-PA Author Manuscript
NIH-PA Author Manuscript
NIH-PA Author Manuscript

Table 3

Weight and dimensional changes of doped, 65-kGy irradiated UHMWPE as a function of temperature

Doping temperature (°C)	Weight change (%)	Volumetric change (%)	Surface VEI	Penetration depth (mm)
100	0.7±0.1	0.4±0.2	0.73±0.10	1.5±0.0
110	1.2 ±0.3	1.1 ±0.1	0.93±0.15	2.5±0.0
120	3.1 ±0.1	3.8 ±0.4	1.38±0.06	3.3±0.3
130	11.6 ±0.2	15.3 ±3.0	3.08±0.10	6.8±0.8
140	28.7 ±1.0	35.0 ±3.4	2.37±0.06	>10

NIH-PA Author Manuscript
NIH-PA Author Manuscript
NIH-PA Author Manuscript

Table 4

Weight and dimensional changes of doped, 100-kGy irradiated UHMWPE as a function of temperature

Doping temperature (°C)	Weight change (%)	Volumetric change (%)	Surface VEI	Penetration depth (mm)
100	1.2±0.0	1.2±0.01	0.66±0.02	1.5±0.2
110	0.7±0.1	0.4±0.3	0.91±0.08	2.0±0.0
120	2.8±0.0	3.5±0.4	1.58±0.10	4.0±0.9
130	10.7±2.1	10.4±0.8	2.61±0.47	8.2±3.3
140	24.6±0.6	31.1±0.6	4.14±0.14	>10

NIH-PA Author Manuscript
NIH-PA Author Manuscript
NIH-PA Author Manuscript

Table 5

Weight and dimensional changes of doped, unirradiated UHMWPE as a function of temperature

Doping temperature (°C)	Weight change (%)	Volumetric change (%)	Surface Vitamin E Index	Penetration depth (mm)
100	1.1 ±0.0	1.2 ±0.1	1.03±0.16	2.0±0.0
110	2.3 ±0.0	2.3 ±0.1	1.45±0.07	3.5±0.5
120	4.7 ±0.0	5.5 ±0.2	2.20±0.09	3.7±1.0
130	41.2 ±0.4	46.8 ±1.2	5.84±0.40	8.7±1.3
140	47.0 ±0.3	54.9 ±5.8	4.26±1.05	>10

NIH-PA Author Manuscript
NIH-PA Author Manuscript
NIH-PA Author Manuscript

Table 6

Diffusion coefficients ($mm^2/s \times 10^6$) of vitamin E in UHMWPE as a function of radition dose and doping temperature

Doping temperature (°C)	UHMWPE		
	Unirradiated	65-kGy irradiated	100-kGy irradiated
100	7.9±6.2	2.2±0.7	3.0±2.2
110	10.9±2.2	9.0±5.3	6.3±0.5
120	23±9.6	18±6.8	24±13
130	38±20	42±25	37±10
140	870±1160	933±379	520±503

NIH-PA Author Manuscript
NIH-PA Author Manuscript
NIH-PA Author Manuscript

Table 7

Impedance values for diffu sion of vitamin E in UHMWPE.

Doping temperature (°C)	UHMWPE		
	Unirradiated	65-kGy irradiated	100-kGy irradiated
100	109	467	173
110	79	104	87
120	38	52	22
130	23	22	14

NIH-PA Author Manuscript

NIH-PA Author Manuscript

NIH-PA Author Manuscript

Table 8

Weight and dimensional changes of doped, 65-kGy irradiated UHMWPE

Doping time (°C)	Weight change (%)	Volumetric change (%)
2 hrs	0.8±0.0	1.1±0.0
26 hrs	2.8±0.1	2.7±0.2

NIH-PA Author Manuscript

NIH-PA Author Manuscript

NIH-PA Author Manuscript

Table 9

Weight and dimensional changes of doped, 100-kGy irradiated UHMWPE

Doping time (°C)	Weight change (%)	Volumetric change (%)
2 hrs	0.7±0.0	−0.3±0.1
26 hrs	3.0±0.1	3.2±0.8